ISSN 1063-7834, Physics of the Solid State, 2013, Vol. 55, No. 12, pp. 2491–2500. © Pleiades Publishing, Ltd., 2013.
Original Russian Text © B.A. Belyaev, A.V. Izotov, 2013, published in Fizika Tverdogo Tela, 2013, Vol. 55, No. 12, pp. 2370–2378.

MAGNETISM

# Micromagnetic Calculation of Magnetostatic Oscillation Modes of an Orthogonally Magnetized Disk of Yttrium Iron Garnet

**B. A. Belyaev[a, b, c, *] and A. V. Izotov[c]**

[a] *Kirensky Institute of Physics, Siberian Branch of the Russian Academy of Sciences, Akademgorodok 50–38, Krasnoyarsk, 660036 Russia*

** e-mail: belyaev@iph.krasn.ru*

[b] *Reshetnev Siberian State Aerospace University, pr. Imeni Gazety "Krasnoyarskii Rabochii" 31, Krasnoyarsk, 660014 Russia*

[c] *Siberian Federal University, pr. Svobodnyi 79, Krasnoyarsk, 660041 Russia*

Received May 14, 2013

**Abstract**—The absorption spectrum of a normally magnetized disk of yttrium iron garnet, which is associated with resonances of magnetostatic oscillation modes excited by a homogeneous high-frequency magnetic field, has been investigated using a numerical analysis of the micromagnetic model developed for ferromagnetic objects. The distribution of magnetization oscillation amplitudes over the disk surface area has been obtained for the first four modes. A good agreement between the results of the micromagnetic simulation and the data of analytical calculations for special cases has proved the reliability and efficiency of the proposed approach in numerical experiments on the study of the magnetization dynamics in objects with different geometries and shapes, including multilayer magnetic film structures.

**DOI:** 10.1134/S1063783413120068

## 1. INTRODUCTION

As is known, the characteristics of microwave devices using magnetic materials as active media depend substantially on the spectrum of natural oscillations of magnetization, which, in turn, is determined by many factors, including the shape of samples and the boundary conditions on the surface. However, the study of the magnetization dynamics in high-frequency and static magnetic fields is also very important for the elucidation of the nature and conditions of the origin of various oscillation modes in complex magnetic structures [1, 2]. These problems are solved using both analytical and numerical methods. Analytical methods are based either on the solution of the classical Walker equation [3, 4], which describes the dynamic variations of the magnetostatic potential in a uniformly magnetized sample, or on the use of tensor Green's functions [5, 6]. Moreover, as a rule, the analytical solution can be obtained only in the case of a homogeneous internal magnetic field in the studied objects; therefore, the samples should have a spherical or ellipsoidal shape. On this basis, in a number of works, exact analytical solutions were obtained for some objects, in particular, for a spheroid, an infinite plate, and an infinite cylinder [7].

However, the most important problem in the development of magnetoelectronic devices is to determine the natural frequencies and natural oscillation modes in actually used ferromagnetic objects of various shapes, for example, disks, cylinders, parallelepipeds, or rings [2], in which the internal magnetic field, as a rule, is highly inhomogeneous even in a uniformly magnetized sample. In this case, inhomogeneities of the internal field in such complex objects are caused by inhomogeneities of the demagnetizing fields, which are generated by surface magnetic charges. Therefore, when studying the magnetization dynamics in samples with inhomogeneous internal fields, which are especially pronounced in objects with sizes of the same order of magnitude in all three coordinates, it is required to know the spatial distribution of the internal field. This substantially complicates the problem, but, in the case of its solutions, makes it possible to reveal new effects, for example, those associated with the localization of oscillation modes in particular areas of the object [8, 9].

The solution of the problem with a required accuracy for magnetic samples of "complex" shapes can be obtained using numerical methods of analysis of their models on the basis of the theory of micromagnetism [10], which are being actively developed in recent years. In [11, 12], the natural frequencies and natural oscillation modes of the magnetization were determined using the standard programs originally developed for the determination of the ground state of the magnetization in the sample. In the solution, the authors used a Fourier analysis of the response of the magnetic system to an applied external field pulse, which was related to the dynamics of chosen magnetization components. The main difficulty of this

approach is associated with the complexity of the formation of an appropriate field pulse, because, by virtue of nonlinearity of the medium at large oscillation amplitudes, the normal modes become coupled, which makes it impossible to resolve them (to separate them from each other).

In recent years, numerical methods for solving this problem have been developed [13–15] and have already been widely used. These methods are based on the linearization of the Landau–Lifshitz equation for the case of small magnetization oscillations with respect to the ground state. The solution of this equation is reduced to the standard problem for eigenvectors and eigenvalues. This idea was implemented in our previous study [16], where we described the approach to the calculation of the normal magnetization oscillation modes and the spin-wave absorption spectrum using the previously developed discrete model of the object under investigation [17, 18].

In this work, the objects of investigation are orthogonally magnetized thin disks of yttrium iron garnet (YIG), which have been used both as active elements in constructions of microstrip devices with controlled characteristics for communication and radar systems and as high-speed actuators of modern magnetic recording and data transmitting systems [2, 19]. It is also important that, for uniformly magnetized disks, there are analytical methods of calculation, which makes it possible not only to perform a comparison, but also to evaluate the accuracy and efficiency of the proposed numerical method of calculation.

## 2. MATHEMATICAL DESCRIPTION OF THE DISCRETE MODEL OF A FERROMAGNET

Let us divide a ferromagnetic object into $N$ identical discrete elements in the form of a parallelepiped with volume $V_0$, where the components of the magnetization $\mathbf{M}^{(i)}$ ($i = 1, 2, ..., N$) are specified in each element. In this case, the expression for the free energy, which includes the Zeeman energy, the energy of exchange and magnetostatic interactions, and the energy of uniaxial magnetic anisotropy, can be written in the form [17]

$$F(\mathbf{M}^{(1)}, \mathbf{M}^{(2)}, ..., \mathbf{M}^{(N)}) = -V_0\sum_{i=1}^{N}\left[\mathbf{H}\mathbf{M}^{(i)} + \frac{1}{2}\sum_{j=1}^{N}\mathbf{M}^{(i)}\overleftrightarrow{A}^{(ij)}\mathbf{M}^{(j)}\right], \quad (1)$$

where $\mathbf{H}$ is the external magnetic field and $\overleftrightarrow{A}^{(ij)}$ is the tensor describing the interaction between the discrete elements $i$ and $j$, which is determined by the internal properties of the studied magnetic system,

$$\overleftrightarrow{A}^{(ij)} = \begin{cases}\overleftrightarrow{A}^{a(ii)} + \overleftrightarrow{A}^{\mathrm{dem}(ii)}, & i = j\\ \overleftrightarrow{A}^{\mathrm{ex}(ij)} + \overleftrightarrow{A}^{\mathrm{dem}(ij)}, & i \neq j.\end{cases} \quad (2)$$

Here, $\overleftrightarrow{A}^{\mathrm{ex}(ij)}$ and $\overleftrightarrow{A}^{a(ij)}$ are the tensors describing respectively the exchange interaction (with the exchange constant $J$) and the magnetic anisotropy (with the uniaxial anisotropy constant $K_i$ and the direction of the easy magnetization axis specified by the unit vector $\mathbf{n}^{(i)}$),

$$\overleftrightarrow{A}^{\mathrm{ex}(ij)} = \frac{2J}{M_s^2}\overleftrightarrow{E}, \quad \overleftrightarrow{A}^{a(ii)} = \frac{2K_i}{M_s^2}\begin{pmatrix} n_x^{(i)} \\ n_y^{(i)} \\ n_z^{(i)}\end{pmatrix}(n_x^{(i)}n_y^{(i)}n_z^{(i)}), \quad (3)$$

where $M_s$ is the saturation magnetization of the sample and $\overleftrightarrow{E}$ is the unit $3 \times 3$ matrix. The magnetostatic energy associated with the dipole–dipole interaction between the discrete elements is described by the tensor $\overleftrightarrow{A}^{\mathrm{dem}(ij)}$. The tensor components, as a rule, are calculated using either exact analytical expressions for discrete elements in the form of a parallelepiped, obtained in [20], or the approximation accounting for the interaction of a pair of point dipoles [17], which adequately describes the interaction of spherical nanoparticles.

In the case of the spatial discretization of the studied object, the effective local magnetic field acting on the magnetization of the $k$th cell has the form

$$\mathbf{H}^{\mathrm{eff}(k)}(\mathbf{M}^{(1)}, \mathbf{M}^{(2)}, ..., \mathbf{M}^{(N)}) = -\frac{1}{V_0}\frac{\delta F}{\delta \mathbf{M}^{(k)}} = \mathbf{H} + \sum_{j=1}^{N}\overleftrightarrow{A}^{(kj)}\mathbf{M}^{(j)}, \quad (4)$$

and the equation of motion of the magnetization of the $k$th cell ($k = 1, ..., N$) is described by the Landau–Lifshitz equation

$$\frac{\partial \mathbf{M}^{(k)}}{\partial t} = -\gamma[\mathbf{M}^{(k)} \times \mathbf{H}^{\mathrm{eff}(k)}] - \gamma\frac{\alpha}{M_s}\mathbf{M}^{(k)} \times [\mathbf{M}^{(k)} \times \mathbf{H}^{\mathrm{eff}(k)}]. \quad (5)$$

Here, the first term describes the precession of the magnetization around the effective local magnetic field $\mathbf{H}^{\mathrm{eff}(k)}$, the second term describes the damping in the system, $\gamma$ is the gyromagnetic ratio, and $\alpha$ is the damping parameter.

Using the method of successive approximations [7] and taking into account the inequalities $|\mathbf{m}^{(k)}| \ll \left|\mathbf{M}_0^{(k)}\right|$ and $|\mathbf{h}^{\text{eff}(k)}| \ll \left|\mathbf{H}_0^{\text{eff}(k)}\right|$, the solution will be sought in the form

$$\begin{aligned} \mathbf{M}^{(k)} &= \mathbf{M}_0^{(k)} + \mathbf{m}^{(k)}(t), \\ \mathbf{H}^{\text{eff}(k)} &= \mathbf{H}_0^{\text{eff}(k)} + \mathbf{h}^{\text{eff}(k)}(t), \end{aligned} \tag{6}$$

where $\mathbf{M}_0^{(k)}$ is the equilibrium magnetization of the $k$th cell, which, as shown in [17], is determined using the system of linear inhomogeneous equations with undetermined Lagrange multipliers $\nu_k$:

$$\mathbf{H}_0^{\text{eff}(k)}(\mathbf{M}_0^{(1)}, \mathbf{M}_0^{(2)}, \ldots, \mathbf{M}_0^{(N)}) - \nu_k \mathbf{M}_0^{(k)} = 0. \tag{7}$$

Earlier [17], we proposed the algorithm for solving such a system of equations. The check for stability of this solution of the system is determined from the requirement of positive determinedness of the matrix $A' = (\overleftrightarrow{A}^{(ij)} - \nu_i \delta_{ij} \overleftrightarrow{E})$, where $\delta_{ij}$ is the Kronecker delta. In this case, in expression (6), $\mathbf{m}^{(k)}(t)$ is the dynamic part of the magnetization, and the static and dynamic parts of the effective field are determined in accordance with formulas (4) and (7) as follows:

$$\begin{aligned} \mathbf{H}_0^{\text{eff}(k)} &= \sum_{i=1}^{N} \overleftrightarrow{A}^{(ki)} \mathbf{M}_0^{(i)} + \mathbf{H}_0 = \nu_k \mathbf{M}_0^{(k)}, \\ \mathbf{h}^{\text{eff}(k)}(t) &= \sum_{i=1}^{N} \overleftrightarrow{A}^{(ki)} \mathbf{m}^{(i)}(t) + \mathbf{h}^{\text{rf}(k)} = \mathbf{j}^{(k)} + \mathbf{h}^{\text{rf}(k)}. \end{aligned} \tag{8}$$

Considering only the linear terms in the equation taking into account that $[M_0^{(k)} \times \mathbf{H}^{\text{eff}(k)}] = 0$, we can write the equation of motion (5) in the form

$$\frac{\partial \mathbf{m}^{(k)}}{\partial t} = \sum_{i=1}^{N} \overleftrightarrow{B}^{(ki)} \mathbf{m}^{(i)} + \overleftrightarrow{N}_0^{(k)} \mathbf{h}^{\text{rf}(k)}. \tag{9}$$

Here, we used the following notation:

$$\begin{aligned} \overleftrightarrow{M}_0^{(k)} &= \begin{pmatrix} 0 & -M_{0z}^{(k)} & M_{0y}^{(k)} \\ M_{0z}^{(k)} & 0 & -M_{0x}^{(k)} \\ -M_{0y}^{(k)} & M_{0x}^{(k)} & 0 \end{pmatrix}, \\ \overleftrightarrow{N}_0^{(k)} &= -\gamma\left(\overleftrightarrow{M}_0^{(k)} - \frac{\alpha}{M_s}(\overleftrightarrow{M}_0^{(k)})^2\right), \\ \overleftrightarrow{B}^{(ki)} &= \overleftrightarrow{N}_0^{(k)}(\overleftrightarrow{A}^{(ki)} - \nu_k \delta_{ki} \overleftrightarrow{E}), \end{aligned} \tag{10}$$

where $M_{0x}^{(k)}$, $M_{0y}^{(k)}$, and $M_{0z}^{(k)}$ are the components of the vector $\mathbf{M}_0^{(k)}$.

In order to determine the normal magnetic modes of magnetization oscillations, we first of all consider the case of free oscillations. In the absence of an external alternating field ($\mathbf{h}^{\text{rf}(k)} = 0$), expression (9) has the simple form

$$\frac{\partial \mathbf{m}^{(k)}}{\partial t} = \sum_{i=1}^{N} \overleftrightarrow{B}^{(ki)} \mathbf{m}^{(i)} \quad (k = 1, 2, \ldots, N). \tag{11}$$

The solution to the system of linear differential equations (11) will be sought in the form of $\mathbf{m}^{(i)}(t) = \mathbf{V}^{(i)} e^{\lambda t}$. Here, $\lambda = -i\omega$; $\omega$ is the precession frequency of the magnetization. After substituting this term into expression (11), we obtain

$$\sum_{i=1}^{N} \overleftrightarrow{B}^{(ki)} \mathbf{V}^{(i)} = \lambda \mathbf{V}^{(k)} \quad (k = 1, 2, \ldots, N). \tag{12}$$

By solving equation (12) for eigenvectors and eigenvalues, the general solution of the homogeneous system (11) can be written as an expansion in eigenvectors of normal magnetic oscillation modes

$$\mathbf{m}^{(i)}(t) = \sum_{m=1}^{M} C_m \mathbf{V}_m^{(i)} e^{\lambda_m t} \quad (i = 1, 2, \ldots, N), \tag{13}$$

where $M$ is the number of oscillation modes taken into account in the calculation ($M \le 2N$); $\lambda_m$ is the eigen number (self-resonant frequency of the mode) corresponding to the eigenvector (column) $\mathbf{V}_m = [\mathbf{V}_m^{(1)}; \mathbf{V}_m^{(2)}; \ldots; \mathbf{V}_m^{(N)}]$; and $\mathbf{V}_m^{(1)}$, $\mathbf{V}_m^{(2)}$, ..., $\mathbf{V}_m^{(N)}$ are the amplitudes of magnetization oscillations in each cell at a frequency of the $m$th mode.

In the case of forced oscillations, we need to solve the inhomogeneous system of equations (9). For this purpose, we use the method of variation of arbitrary constants, i.e., the solution will be sought in the form

$$\mathbf{m}^{(i)}(t) = \sum_{m=1}^{M} C_m(t) \mathbf{V}_m^{(i)} e^{\lambda_m t} \quad (i = 1, 2, \ldots, N). \tag{14}$$

By substituting this expression into the system of equations (9), we obtain

$$\sum_{m=1}^{M} \mathbf{V}_m^{(k)} e^{\lambda_m t} \frac{\partial C_m(t)}{\partial t} = \overleftrightarrow{N}_0^{(k)} \mathbf{h}^{\text{rf}(k)} \quad (k = 1, 2, \ldots, N). \tag{15}$$

In order to solve this system of equations, we introduce the following notation:

$$V = \begin{bmatrix} \mathbf{V}_1^{(1)} & \mathbf{V}_2^{(1)} & \dots & \mathbf{V}_M^{(1)} \\ \mathbf{V}_1^{(2)} & \mathbf{V}_2^{(2)} & \dots & \mathbf{V}_M^{(2)} \\ \dots & \dots & \dots & \dots \\ \mathbf{V}_1^{(N)} & \mathbf{V}_2^{(N)} & \dots & \mathbf{V}_M^{(N)} \end{bmatrix},$$
$$U = \begin{bmatrix} \mathbf{U}_1^{(1)} & \mathbf{U}_1^{(2)} & \dots & \mathbf{U}_1^{(N)} \\ \mathbf{U}_2^{(1)} & \mathbf{U}_2^{(2)} & \dots & \mathbf{U}_2^{(N)} \\ \dots & \dots & \dots & \dots \\ \mathbf{U}_M^{(1)} & \mathbf{U}_M^{(2)} & \dots & \mathbf{U}_M^{(N)} \end{bmatrix}, \quad UV = E, \tag{16}$$

where $E$ is the identity matrix and $U = (V^T V)^{-1} V^T$ (here, $T$ denotes the transposition, and $-1$ indicates the inverse matrix). It should be specially noted that the solution of equation (12) leads to a complex conjugate eigenvalue pairs $\lambda_m$ and $\lambda_m^*$ and their corresponding eigenvector pairs $\mathbf{V}_m$ and $\mathbf{V}_m^*$, which, in turn, are not linearly independent (their real and imaginary parts are linearly independent). Therefore, the product $V^T V$ is not the identity matrix and $U \neq V^T$.

With this notation, the system of equations (15) is reduced to the following form:

$$\frac{\partial C_m(t)}{\partial t} = e^{-\lambda_m t} \sum_{j=1}^{N} \mathbf{U}_m^{(j)} \overleftrightarrow{N}_0^{(j)} \mathbf{h}^{\mathrm{rf}(j)} \quad (m = 1, 2, \dots, M). \tag{17}$$

By integrating the differential equations, we find

$$C_m(t) = C_m^{\mathrm{free}} + \int e^{-\lambda_m t} \sum_{j=1}^{N} \mathbf{U}_m^{(j)} \overleftrightarrow{N}_0^{(j)} \mathbf{h}^{\mathrm{rf}(j)} dt. \tag{18}$$

This expression determines the oscillation amplitude of the $m$th mode upon excitation of the system by a high-frequency field of any form; however, from the practical point of view, it is important to consider the case of excitation of the system by a high-frequency sinusoidal field $\mathbf{h}^{\mathrm{rf}(j)}(t) = \mathbf{h}_0^{\mathrm{rf}(j)} e^{-i\omega t}$ with a frequency $\omega$. Then, the expression defining the mode amplitudes takes the form

$$C_m(t) = C_m^{\mathrm{free}} + \frac{e^{-(\lambda_m + i\omega)t}}{-(\lambda_m + i\omega)} \sum_{j=1}^{N} \mathbf{U}_m^{(j)} \overleftrightarrow{N}_0^{(j)} \mathbf{h}_0^{\mathrm{rf}(j)}. \tag{19}$$

By substituting this expression into formula (14), we obtain the general solution of the equation describing the motion of the magnetization of the $i$th cell:

$$\mathbf{m}^{(i)}(t) = \sum_{m=1}^{M} C_m^{\mathrm{free}} \mathbf{V}_m^{(i)} e^{\lambda_m t} + \sum_{m=1}^{M} \sum_{j=1}^{N} \frac{\mathbf{U}_m^{(j)} \overleftrightarrow{N}_0^{(j)} \mathbf{h}_0^{\mathrm{rf}(j)}}{-(\lambda_m + i\omega)} \cdot \mathbf{V}_m^{(i)} e^{-i\omega t}. \tag{20}$$

It should be noted that the first term of this expression describes free oscillations of the magnetic system. This can be easily seen if we put $\mathbf{h}_0^{\mathrm{rf}(j)}$ equal to zero. In the case of the damping in the system, the behavior of $\mathbf{m}^{(i)}(t)$ in the steady-state regime is described by the expression

$$\mathbf{m}^{(i)}(t) = \sum_{m=1}^{M} \sum_{j=1}^{N} \frac{\mathbf{U}_m^{(j)} \overleftrightarrow{N}_0^{(j)} \mathbf{h}_0^{\mathrm{rf}(j)}}{-(\lambda_m + i\omega)} \cdot \mathbf{V}_m^{(i)} e^{-i\omega t}. \tag{21}$$

In this case, we can easily calculate the absorption energy of the high-frequency field [21]

$$E = \omega V_0 \sum_{i=1}^{N} \mathrm{Im}[\mathbf{m}^{(i)} \mathbf{h}^{\mathrm{rf}(i)*}]. \tag{22}$$

The obtained expressions allow one to examine the dynamics of a magnetic system in ferromagnetic samples of any desired shape, including multilayer film structures. They make it possible to investigate not only the regularities in the behavior of the spectra of natural modes of magnetization oscillations by varying the parameters of the studied object, but also the location and spatial distribution of the magnetization oscillation amplitudes for different modes, as well as the frequency and field dependences of the magnetic permeability.

## 3. RESULTS OF THE NUMERICAL SIMULATION

In this work, we have calculated the magnetostatic oscillation modes of the magnetization and the high-frequency absorption spectrum of a thin disk magnetized orthogonally to the plane by an external static magnetic field $H_0$ to saturation. In order to compare our results with the data obtained in other works, we chose the disk with diameter $D = 2R = 3.98$ mm and thickness $L = 0.284$ mm, i.e., with the ratio $L/D = 0.0714$. The magnetic parameters of the disk correspond to iron yttrium ferrite with a structure of the $Y_3Fe_5O_{12}$ garnet, which has the saturation magnetization $M_s = 149.6$ G, the exchange constant $A = Jd^2 = 0.425 \times 10^{-6}$ erg/cm ($d$ is the distance between the adjacent discrete elements), and the damping coefficient of the magnetization precession $\alpha = 0.0005$. It should be noted that, in this problem, the crystallo-

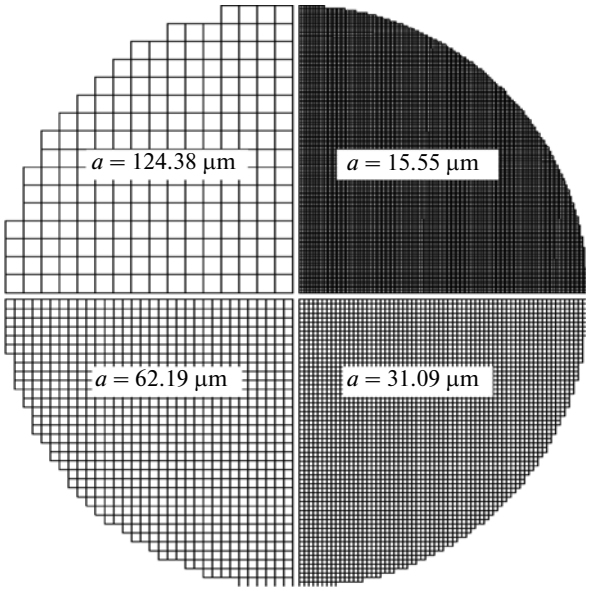


**Fig. 1.** Fragments of the models of the studied disk after discretization in the plane by square grids with different steps.

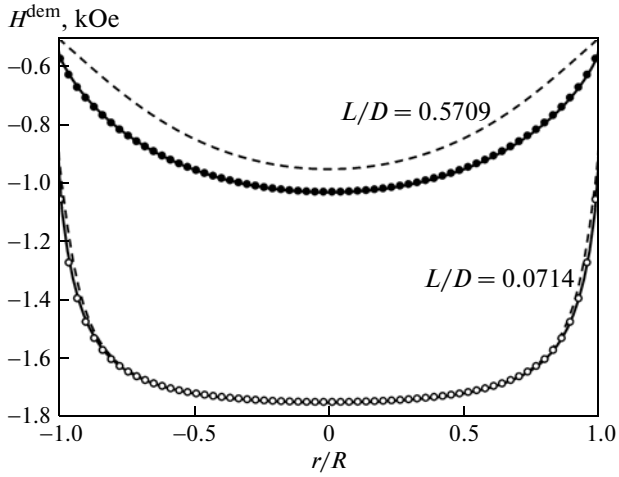


**Fig. 2.** Dependences of the demagnetizing fields $H^{dem}(r)$ along the diameter of the orthogonally magnetized YIG disk for two values of the ratio $L/D$. Open and closed circles indicate the results of the numerical calculation of the discrete model for $a = 62.19$ μm. Solid and dashed lines correspond to the analytical calculations according to formulas from [24] and [23], respectively.

graphic magnetic anisotropy of the sample was not considered to facilitate the analysis of the results.

The discretization of the studied disk was performed only in the plane; in this case, we used four different square grids with a multiple decrease in the size of cells, which, with two decimal places, had the following values: $a = 124.38$, 62.19, 31.09, and 15.55 μm (Fig. 1). This was necessary to evaluate the influence of the degree of discretization on the quality of the numerical calculation. As a result, the sample was divided into equal parallelepipeds $a \times a \times L$ in size. Because of the strong influence of the shape anisotropy, for the chosen geometry of the "unit cell" in our calculation of the magnetostatic interaction tensor, we used the exact analytical expression presented in [20]. The external static magnetic field $H_0 = 4.9$ kOe, which was applied orthogonally to the film plane, obviously, ensured the reliable homogeneous "magnetization" of the sample.

First of all, we consider the results of the numerical simulation of the demagnetizing field, which exerts a significant influence on the high-frequency properties of magnetic disks. In the framework of the considered discrete model, the demagnetizing field was defined by the following expression:

$$\mathbf{H}^{\mathrm{dem}(i)} = -\sum_{j=1}^{N} \overleftrightarrow{A}^{\mathrm{dem}(ij)} \mathbf{M}_0^{(j)}, \qquad (23)$$

where $\mathbf{M}_0^{(j)}$ is the equilibrium magnetization of the $j$th cell. It should be noted that the algorithm for calculating the demagnetizing fields included the method of fast Fourier transform [22], which made it possible to decrease the required memory for storing the elements $\overleftrightarrow{A}^{\mathrm{dem}(ij)}$ and to significantly speed up the computational procedures.

The results of the numerical calculation of the dependence of the demagnetizing field $H^{dem}$ on the coordinate $r$ along the diameter of the studied disk with the discretization cell size $a = 62.19$ μm are shown by open circles in Fig. 2. For comparison, closed circles in this figure show a similar dependence constructed for the disk with the ratio $L/D = 0.5709$. Dashed lines represent the results of the calculation according to the formula $H^{dem}(r) = -4\pi M_s I(r)$, for which the dependence of the demagnetizing factor $I(r)$ was obtained analytically in the approximation $L/D \ll 1$ [23].

It can be seen that, for the studied disk ($L/D = 0.0714$), the discrepancy between the results of the micromagnetic simulation and analytical calculation is noticeable only at the edges of the sample; however, for the disk with $L/D = 0.5709$, this discrepancy is significant for any $r$. Solid lines in the figure show the dependences constructed using a more accurate analytical expression for the demagnetizing factor $I(r) = N_{zz}(r, z)$ [24], which also takes into account the dependence of the demagnetizing factor on the thickness of the sample. These results agree very well with the results of the numerical simulation both in the case of $L/D = 0.0714$ and in the case of $L/D = 0.5709$.

It is important to note that, in uniformly magnetized samples of nonellipsoidal shape, the inhomoge-

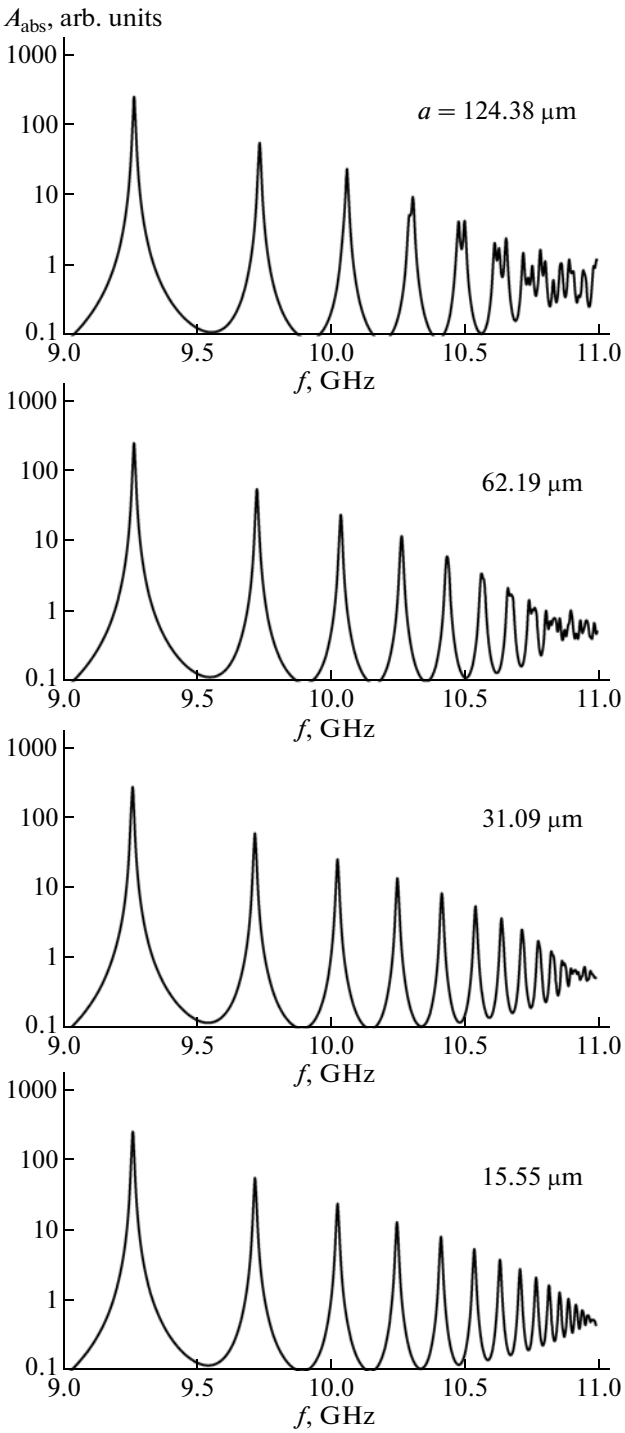


**Fig. 3.** Resonance absorption spectra constructed for a normally magnetized YIG disk upon pumping by a homogeneous external high-frequency field in the plane for different sizes of elements in the discrete model.

neous internal magnetic field can encourage excitation of magnetostatic oscillation modes under the influence of a homogeneous high-frequency magnetic field, which was observed for the first time by Dillon [25]. This fact is well illustrated by the numerical calculation of the absorption spectrum of the studied YIG disk in the microwave range, which was performed using the discrete model and the derived expression (22).

Figure 3 shows four microwave absorption spectra calculated for different discretizations. It can be seen that the part of the spectrum in the regions of lower oscillation modes remains almost unchanged with a decrease in the cell size $a$ from 124.38 to 15.55 μm. However, as should be expected, the division of the disk into "large" discrete elements leads to an ambiguous determination of higher oscillation modes, so that their spectrum in this case has a number of additional resonances. It can be seen that, with an increase in the number of elements in the discrete model, the spectrum in the region of higher modes of inhomogeneous magnetization oscillations is gradually "purified" from additional resonances, but, accordingly, this leads to an increase in the required computational time [22]. Therefore, for each studied method of micromagnetic simulation of the object, it is important to determine the optimum discretization of the model. Our estimates show that, for a satisfactory description of the spectrum in the frequency range studied, it is required that the wavelength of the highest oscillation modes in the spectrum should be accounted for by at least ten discrete cells.

In order to estimate the accuracy of the calculation of the microwave absorption spectra, we compare the results of our simulation with the results of the calculation in the model proposed by Yukawa and Abe [23], which is simple but quite well consistent with the experiment. In this model, the dispersion relation for magnetostatic waves in a normally magnetized plate or disk was obtained at standard electrodynamic boundary conditions on the upper and lower surfaces of the sample [7]:

$$\sqrt{-\mu}\tan(\sqrt{-\mu}kL/2) = 1. \quad (24)$$

Here, $k$ is the wave number of a magnetostatic wave propagating in the plane of the disk and μ is the diagonal component of the magnetic permeability tensor

$$\overleftrightarrow{\mu} = \begin{bmatrix} \mu & i\mu_a & 0 \\ -i\mu_a & \mu & 0 \\ 0 & 0 & 1 \end{bmatrix}, \quad (25)$$

where

$$\mu = \frac{H_i B_i - (\omega/\gamma)^2}{H_i^2 - (\omega/\gamma)^2}, \quad \mu_a = \frac{4\pi M_s(\omega/\gamma)}{H_i^2 - (\omega/\gamma)^2},$$

$H_i(r) = H_0 - 4\pi M_s I(r)$ is the internal magnetic field of the disk and $B_i(r) = H_i(r) + 4\pi M_s$.

An important condition for the existence of bulk magnetostatic waves, according to dispersion relation (24), is the requirement $\mu < 0$, which determines the

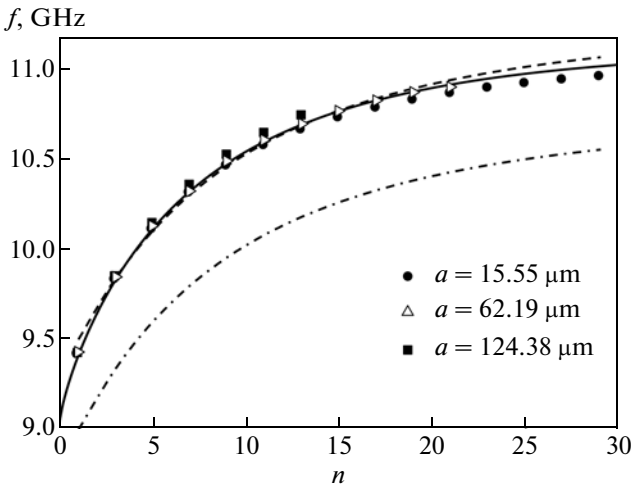


**Fig. 4.** Dependences of the natural magnetostatic oscillation frequencies for an orthogonally magnetized disk on the mode number. Points are the results of the numerical simulation, the solid lines show the results of the calculations in the model of Yukawa and Abe, and the dashed and dash-dotted lines correspond to the calculations [26] with and without averaging of the demagnetizing factor, respectively.

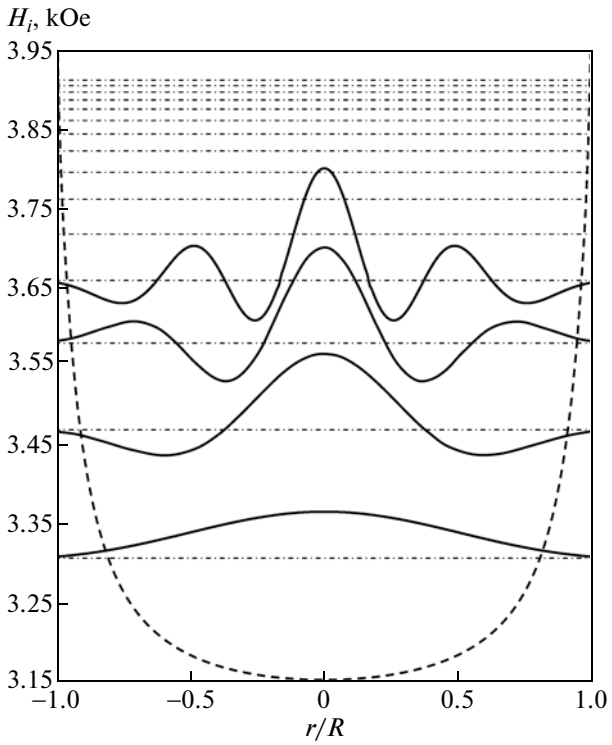


**Fig. 5.** Distribution of the internal magnetic field $H_i(\rho)$ over the disk diameter (dashed line) and the resonance fields $\omega_{res}/\gamma$ (dash-dotted horizontal lines). Solid lines show the distributions of the high-frequency magnetization oscillation amplitudes for the four lowest modes constructed on this figure for clarity in arbitrary units.

cutoff frequencies of magnetostatic waves $H_i(r) \le \omega/\gamma \le \sqrt{H_i(r)B_i(r)}$. The magnetostatic wave propagating in the inhomogeneous internal field $H_i(r)$ radially from the center of the disk undergoes reflection at a specific distance $r_1$, where the wave number $k$ vanishes. For $r > r_1$, the wave number in the general case becomes complex, which corresponds to oscillations with an exponentially decreasing amplitude. The distance $r_1$, at which there occurs a reflection of the magnetostatic wave, is determined from the condition $\omega/\gamma = H_i(r_1)$.

The condition of a standing wave, when an integer number of half-waves fits at the distance $-r_1 < r < r_1$, leads to the expression for calculating the number $n$ of the magnetostatic oscillation mode. Using the designations $\rho = r/R$ and $\rho_1 = r_1/R$, we can write the above condition in the form [23]

$$n = \frac{2}{\pi}\frac{D}{L}\int_0^{\rho_1}\frac{1}{\sqrt{-\mu}}\tan^{-1}\frac{1}{\sqrt{-\mu}}d\rho. \qquad (26)$$

Every time when $n$ becomes an integer, there occurs a resonant absorption of the high-frequency pump field energy. It should be recalled that, when the sample is placed in a homogeneous high-frequency magnetic field, magnetostatic oscillations are excited only for odd mode numbers $n$. As was shown by Yukawa and Abe, the theoretical results obtained using expressions (26) are in quite good agreement with experimental measurements [23].

The dependence of the natural magnetostatic oscillation frequencies on the mode number calculated for an orthogonally magnetized disk according to formula (26) is shown by the solid line in Fig. 4. In this case, the internal field $H_i(r)$ involved in the expression for the magnetic permeability $\mu$ was determined using an improved analytical calculation of the demagnetizing factor [24]. The points in the figure represent the results of the numerical micromagnetic calculation performed for three different cell sizes in the discrete model. It can be seen that the resonant frequencies of the lowest oscillation modes obtained by the numerical calculation are in good agreement with the results of the analytical calculation for any degree of discretization of the model. However, in the region of higher modes, there is some difference. In the numerical calculations for the model with $a = 124.38$ μm, the insufficient degree of discretization of the disk is the cause for the overestimation of the frequency of higher modes in comparison with the analytical calculation. However, at a sufficiently high discretization of the disk ($a = 15.55$ μm), the numerical calculation, on the contrary, gives a small decrease in the resonant frequencies of the higher oscillation modes. The discrepancy between the analytical calculation and the

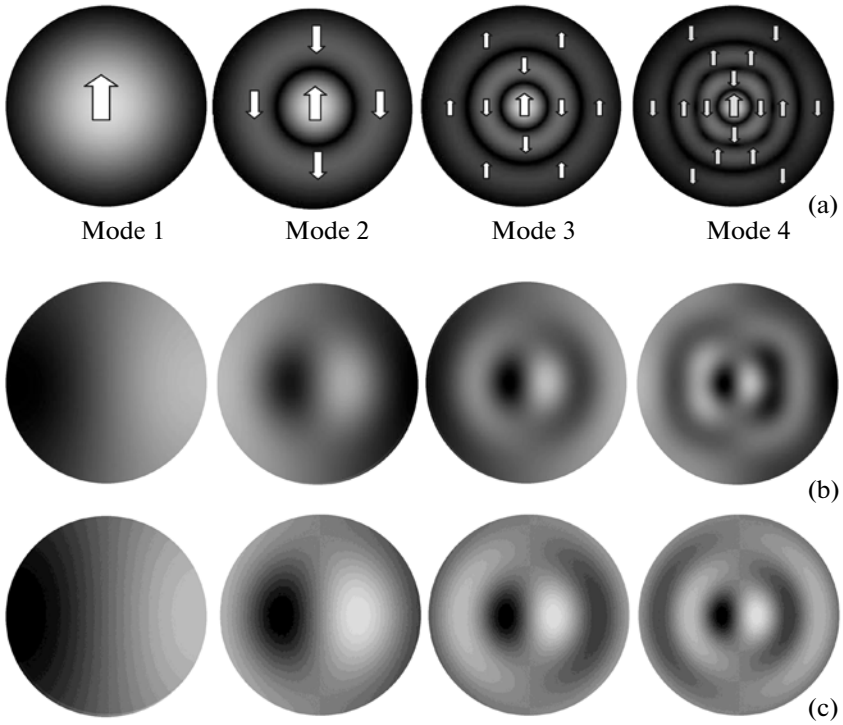


**Fig. 6.** (a) Distribution of the magnetization oscillation amplitudes for the four lowest modes (arrows indicate the directions of the magnetization motion at a fixed point of time) and (b, c) distributions of the magnetostatic potential for the first four modes according to (b) results of the numerical simulation and (c) results of the calculation using formula (27).

numerical calculation in the discrete model can be understood from Fig. 5.

In Fig. 5, the dashed line shows the distribution of the internal magnetic field $H_i(\rho)$ along the diameter of the disk, and the dash-dotted horizontal lines indicate values of the resonance fields $\omega_{res}/\gamma$ for the observed magnetization oscillation modes. Moreover, for the four lowest resonant modes, this figure shows the calculated distributions of the high-frequency magnetization oscillation amplitudes. It can be seen that the boundaries of the existence of the magnetostatic modes $-r_1 < r < r_1$, which are used in the theoretical model proposed by Yukawa and Abe, do not localize it completely (at the boundaries, the high-frequency magnetization is nonzero). The magnetization oscillation amplitude exponentially decreasing toward the edges of the disk broadens this region, which leads to an increase in the effective radius for the formation of standing waves and, consequently, to a decrease in the frequency. And since the broadening of the region particularly strongly affects the "short" waves with large values of $k$, the observed difference in the resonant frequencies of the modes increases for peaks with a large value of $n$.

The analytical model proposed by Yukawa and Abe, despite its simplicity and good agreement with the experiment, cannot completely meet all the needs in the analysis of such systems. First, this model is restricted to considering only the radial modes excited by a planar field. The modes, which, in the general case, depend on the azimuthal and normal coordinates, remain beyond the scope of this model. Second, this model does not give an accurate distribution of the excited high-frequency magnetization modes in the sample. Apart from the positions of the absorption peaks and their number, no additional information in the context of this model can be obtained.

The problem of excitation of magnetostatic oscillations in a normally magnetized disk has an exact analytical solution, provided that the internal magnetic field of the disk remains homogeneous [4, 7]. In this case, it is assumed that $I(r) = \text{const}$, and the consideration of the standard electrodynamic boundary conditions on the side surfaces of the disk for the magnetostatic potential

$$\psi(r, \theta, z) = C_m J_m\left(\frac{kr}{\sqrt{-\mu}}\right)\left(\cos kz + \frac{1}{\sqrt{-\mu}}\sin kz\right)e^{-im\theta} \quad (27)$$

leads to the additional equation

$$\sqrt{-\mu}\frac{J'_m(kR/\sqrt{-\mu})}{J_m(kR/\sqrt{-\mu})} + \frac{K'_m(kR)}{K_m(kR)} - \frac{\mu_a m}{kR} = 0, \quad (28)$$

which, together with dispersion relation (24), determines the entire spectrum of magnetostatic oscillations of an orthogonally magnetized disk. Here, $J_m$ is the Bessel function; $K_m$ is the Bessel function of the

imaginary argument; and the factor $C_m$ in formula (27) is the normalization factor, which in our calculations is set equal to unity.

Based on the simultaneous solution of equations (24) and (28) for $I(r) = 1$, in Fig. 4 we plotted the dependence of the resonant frequency on the oscillation mode number $n$ (dash-dotted line). It can be seen that the disregard of the inhomogeneity of the internal field leads to a serious error. To avoid this discrepancy, the authors of [26] proposed to use the method of averaging the demagnetizing factor $I(r)$ along the diameter of the disk and obtained the value $I_{av} \approx 0.895$. Using this value, we carried out the calculation similar to that performed previously. The results of this calculation are presented in Fig. 4 by the dashed line. It can be seen that the results obtained for the lower modes are in good agreement with both the results of the numerical simulation and the results of the calculation in the model proposed by Yukawa and Abe. However, in the cited paper [26], probably, there is some inaccuracy. The average value of the demagnetizing factor $I_{av} \approx 0.895$, which is presented in [26] and obtained for parameters of the model similar to that studied in our work, is slightly overestimated. Indeed, according to [23], this average value is $I_{av} = 0.8714$, but, according to [24], it is $I_{av} = 0.8763$. Possibly, the authors of [26] performed the averaging not over the entire disk width, but only over its part.

For the analysis of the structure of magnetostatic oscillation modes, Fig. 6a presents the distributions of high-frequency magnetization oscillation amplitudes for the four lowest excited modes according to the results of the numerical micromagnetic simulation. Moreover, arrows in this figure schematically indicate the directions of magnetization motion at a fixed point of time. It can be seen that the modes have a strictly radial distribution of the high-frequency magnetization oscillation amplitudes.

Using the results of the numerical simulations, we also obtained the distributions of the magnetostatic potential for these modes (Fig. 6b), which were compared with the results of analytical calculations using formula (27) (Fig. 6c). It can be seen that the obtained results are in very good agreement. A small difference is that the results of the numerical simulation are characterized by a certain localization of the modes closer to the center, which is apparently caused by the inclusion of the inhomogeneity of the internal field, whereas in accordance with formula (27), the modes are more uniformly distributed. Moreover, the results of the numerical simulation demonstrate that the magnetostatic potential for mode 4 begins to show a symmetry that is characteristic of square samples rather than of disks. This is obviously associated with the error in the approximation of the cylindrical surface of the disk by parallelepipeds of insufficiently small sizes.

## 4. CONCLUSIONS

Thus, the absorption spectrum of a normally magnetized disk of yttrium iron garnet has been numerically investigated using the developed micromagnetic model of a ferromagnet. It has been shown that nonuniform magnetostatic oscillations that are responsible for the resonance peaks observed in the absorption spectrum are excited because of the gradient distribution of the internal magnetic field in a magnetized disk, which is subjected to a homogeneous high-frequency magnetic field. A comparison of the results of the micromagnetic simulation with analytical calculations performed for special cases has proved the validity and high reliability of the developed approach to the numerical micromagnetic simulations of ferromagnetic objects with arbitrary shape and size.

It is important to note that the presented calculation allows one not only to determine the spectrum of normal oscillation modes of the magnetization for composite samples of magnetic and nonmagnetic materials of any shape, but also to calculate the electromagnetic energy absorption spectrum for both the magnetic field sweep and the pump frequency sweep. In particular, the developed method makes it possible to investigate the frequency and field dependences of the magnetic permeability tensor components for complex multilayer structures, which are currently considered as the most promising objects for the creation of new microelectronic elements.

## ACKNOWLEDGMENTS

This study was supported by the Ministry of Education and Science of the Russian Federation (state contract no. 14.513.11.0010), the Federal Target Program "Scientific and Scientific–Pedagogical Human Resources for the Innovative Russia in 2009–2013," and the Siberian Branch of the Russian Academy of Sciences (integration project no. 109).

## REFERENCES

1. J. W. Lau and J. M. Shaw, J. Phys. D: Appl. Phys. **44**, 303001 (2011).
2. R. D. McMichael and M. D. Stiles, J. Appl. Phys. **97**, 10J901 (2005).
3. L. R. Walker, Phys. Rev. **105** (2), 390 (1957).
4. E. O. Kamenetskii, Phys. Rev. E: Stat., Nonlinear, Soft Matter Phys. **63**, 066612 (2001).
5. B. A. Kalinikos and A. N. Slavin, J. Phys. C: Solid State Phys. **19**, 7013 (1986).
6. K. Y. Guslienko and A. N. Slavin, J. Appl. Phys. **87**, 6337 (2000).
7. A. G. Gurevich and G. A. Melkov, *Magnetization Oscillations and Waves* (Fizmatlit, Moscow, 1994; CRC, Boca Raton, Florida, United States, 1996).
8. K. Y. Guslienko, R. W. Chantrell, and A. N. Slavin, Phys. Rev. B: Condens. Matter **68**, 024422 (2003).

9. I. Lee, Y. Obukhov, G. Xiang, A. Hauser, F. Yang, P. Banerjee, D. V. Pelekhov, and P. C. Hammel, Nature (London) **466**, 845 (2010).
10. W. F. Brown, *Micromagnetics* (Wiley, New York, 1963; Nauka, Moscow, 1979).
11. J. C. Toussaint, A. Marty, N. Vukadinovic, J. B. Youssef, and M. Labrune, Comput. Mater. Sci. **24**, 175 (2002).
12. M. Grimsditch, G. K. Leaf, H. G. Kaper, D. A. Karpeev, and R. E. Camley, Phys. Rev. B: Condens. Matter **69**, 174428 (2004).
13. K. Rivkin and J. B. Ketterson, J. Magn. Magn. Mater. **306**, 204 (2006).
14. M. Grimsditch, L. Giovannini, F. Monotcello, F. Nizzoli, G. K. Leaf, and H. G. Kaper, Phys. Rev. B: Condens. Matter **70**, 054409 (2004).
15. M. Aquinoa, C. Serpico, G. Miano, G. Bertotti, and I. D. Mayergoyz, Physica B (Amsterdam) **403**, 242 (2008).
16. A. V. Izotov and B. A. Belyaev, Russ. Phys. J. **53** (9), 900 (2011).
17. B. A. Belyaev, A. V. Izotov, and An. A. Leksikov, Phys. Solid State **52** (8), 1664 (2010).
18. A. V. Izotov, B. A. Belyaev, and An. A. Leksikov, Zh. Sib. Fed. Univ., Ser. Mat. Fiz. **3** (1), 64 (2010).
19. B. Pigeau, G. De Loubens, O. Klein, A. Riegler, F. Lochner, G. Schmidt, L. W. Molenkamp, V. S. Tiberkevich, and A. N. Slavin, Appl. Phys. Lett. **96**, 132506 (2010).
20. A. J. Newell, W. Williams, and D. J. Dunlop, J. Geophys. Res. [Solid Earth Planets] **98** (B6), 9551 (1993).
21. L. D. Landau and E. M. Lifshitz, *Course of Theoretical Physics*, Vol. 8: *Electrodynamics of Continuous Media*, 2nd ed. (Nauka, Moscow, 1982; Butterworth–Heinemann, Oxford, 1984).
22. A. V. Izotov, B. A. Belyaev, M. M. Valikhanov, S. V. Polenga, and A. V. Stefanyuk, Vychisl. Metody Program. **13** (1), 551 (2012). http://num-meth.srcc.msu.ru/.
23. T. Yukawa and K. Abe, J. Appl. Phys. **45**, 3146 (1974).
24. R. I. Joseph and E. Schlömann, J. Appl. Phys. **36**, 1579 (1965).
25. J. F. Dillon, J. Appl. Phys. **31**, 1605 (1960).
26. E. O. Kamenetskii, R. Shavit, and M. Sigalov, J. Appl. Phys. **95**, 6986 (2004).

*Translated by O. Borovik-Romanova*